ADP-AT-98-9

Acceleration and Interaction of Ultra High Energy Cosmic Rays

R.J. Protheroe

Department of Physics and Mathematical Physics
The University of Adelaide, Adelaide, Australia 5005

Abstract

In this chapter I give an overview of shock acceleration, including a discussion of the maximum energies possible and the shape of the spectrum near cut-off, interactions of high energy cosmic rays with, and propagation through, the background radiation, and the resulting electron-photon cascade. Possible sources of the highest energy cosmic rays are discussed including active galaxies, gamma ray bursts and topological defects. I argue that while the origin of the highest energy cosmic rays is still uncertain, it is not necessary to invoke exotic models such as emission by topological defects to explain the existing data. It seems likely that shock acceleration at Fanaroff-Riley Class II radio galaxies can account for the existing data. However, new cosmic ray data, as well as better estimates of the extragalactic radiation fields and magnetic fields will be necessary before we will be certain of the origin of the highest energy particles occurring in nature.

1. Introduction

Cosmic rays with energies up to 100 TeV are thought to arise predominantly through shock acceleration by supernova remnants (SNR) in our Galaxy (Lagage & Cesarsky 1983). A fraction of the cosmic rays accelerated should interact within the supernova remnant and produce γ–rays (Drury et al. 1994, Gaisser et al. 1998, Baring et al. 1999) , and recent observations above 100 MeV by the EGRET instrument on the Compton Gamma Ray Observatory have found γ-ray signals associated with at least two supernova remnants – IC 443 and γ Cygni (Esposito et al. 1996). However, Brazier et al. (1996) have suggested that the γ-ray emission from IC 443 may be associated with a pulsar within the remnant rather than the remnant itself. Further evidence for acceleration in SNR comes from the Rossi X-ray Timing Explorer observations of Cassiopeia A showing a non-thermal component in the spectrum (Allen et al. 1997), and the ASCA observation of non-thermal X–ray emission from SN 1006 (Koyama et al. 1995). Reynolds (1996) and Mastichiadis (1996) interpret the latter as synchrotron emission by electrons accelerated in the remnant up to energies as high as 100 TeV, although Donea and Biermann (1998) suggest it may be bremsstrahlung from much lower energy electrons. The CANGAROO telescope appears to have detected TeV γ-rays from SN1006 (Tanimori et al. 1998), while there has been a disappointing lack of detections of TeV γ-rays from IC443 and γ Cygni. This may be related to the matter density in which the SNR shocks propagate (Baring et al. 1999), higher densities yielding lower cut-off energies for IC443 and γ Cygni.

Acceleration to somewhat higher energies than 100 TeV may be possible (Markiewicz et al. 1990), but probably not to high enough energies to explain the smooth extension of the spectrum to 1 EeV. Several explanations for the origin of the cosmic rays in this energy range have been suggested: reacceleration of the supernova component while still inside the remnant (Axford 1991); by several supernovae exploding into a region evacuated by a pre-supernova star (Ip and Axford 1991); or acceleration in shocks inside the strong winds from hot stars or groups of hot stars (Biermann and Cassellini 1993). Very recently, an analysis of arrival direction data from AGASA (Hayashida et al. 1998) shows excesses in the directions of the Galactic Centre and the Cygnus region which could not easily be explained by charged particle propagation from these sources. If indeed the excess is due to these sources it may provide some evidence for a component of the cosmic rays at 1 EeV being neutrons. At 5 EeV the spectral slope changes, and there is evidence for a lightening in composition (Bird et al. 1994, Dawson et al. 1998) and it is likely this marks a change from galactic cosmic rays to extragalactic cosmic rays being dominant.

An alternative, although less popular, scenario is that almost all cosmic ray nuclei are of extragalactic origin (e.g. Brecher and Burbidge 1972, and references therein). In any case, whether or not the lower energy cosmic rays are indeed galactic, at the highest energies (above $\sim 10^{19}$ eV) it is very probably extragalactic.

The cosmic ray air shower events with the highest energies so far detected have energies of 2×10^{11} GeV (Hayashida et al. 1994) and 3×10^{11} GeV (Bird et al. 1995), and recent results from AGASA have shown there to be a continuous spectrum between 10^{11} GeV and 3×10^{11} GeV (Takeda et al. 1998)). The question of the origin of these cosmic rays having energy significantly above 10^{11} GeV is complicated by propagation of such energetic particles through the Universe. Nucleons interact with the cosmic background radiation fields, losing energy by Bethe-Heitler pair production, or interacting by pion photoproduction, and in the latter case

may emerge as either protons or neutrons with reduced energy. The threshold for pion photoproduction on the microwave background is $\sim 2\times10^{10}$ GeV, and at 3×10^{11} GeV the energy-loss distance is about 20 Mpc. Propagation of cosmic rays over substantially larger distances gives rise to a cut-off in the spectrum at $\sim 10^{11}$ GeV as was first shown by Greisen (1966), and Zatsepin and Kuz'min (1966), the "GZK cut-off", and a corresponding pile-up at slightly lower energy (Hill and Schramm 1985, Berezinsky and Grigor'eva 1988). These processes occur not only during propagation, but also during acceleration, and may actually limit the maximum energies particles can achieve.

In this chapter I give an overview of shock acceleration, describe interactions of high energy protons and nuclei with radiation, discuss maximum energies obtainable during acceleration, and the shape of the spectrum near maximum energy, outline propagation of cosmic rays through the background radiation and the consequent electron-photon cascading, and finally discuss conventional and exotic models of the highest energy cosmic rays.

2. Interactions of High Energy Cosmic Rays

Interactions of cosmic rays with radiation are important both during acceleration when the resulting energy losses compete with energy gains by, for example, shock acceleration, and during propagation from the acceleration region to the observer. For ultra-high energy (UHE) cosmic rays, the most important processes are pion photoproduction and Bethe-Heitler pair production both on the microwave background, and synchrotron radiation. In the case of nuclei, photodisintegration on the microwave background is important. In this section, I shall describe how to calculate the mean free path for such interactions, and briefly discuss how to simulate the interactions using the Monte Carlo method.

2.1. Nucleons

The mean interaction length, $x_{p\gamma}$, of a proton of energy E is given by,

$$\frac{1}{x_{p\gamma}(E)} = \frac{1}{8\beta E^2}\int_{\varepsilon_{\min}(E)}^{\infty}\frac{n(\varepsilon)}{\varepsilon^2}\int_{s_{\min}}^{s_{\max}(\varepsilon,E)}\sigma(s)(s-m_p^2c^4)dsd\varepsilon, \quad (1)$$

where $n(\varepsilon)$ is the differential photon number density of photons of energy ε, and $\sigma(s)$ is the appropriate total cross section for the process in question for a centre of momentum (CM) frame energy squared, s, given by

$$s = m_p^2c^4 + 2\varepsilon E(1-\beta\cos\theta) \quad (2)$$

where θ is the angle between the directions of the proton and photon, and βc is the proton's velocity.

For pion photoproduction

$$s_{\min} = (m_pc^2 + m_\pi c^2)^2 \approx 1.16\ \mathrm{GeV}^2, \quad (3)$$

and

$$\varepsilon_{\min} = \frac{m_\pi c^2(m_\pi c^2 + 2m_pc^2)}{2E(1+\beta)} \approx \frac{m_\pi c^2(m_\pi c^2 + 2m_pc^2)}{4E}. \quad (4)$$

For photon-proton pair-production the threshold is somewhat lower,

$$s_{\min} = (m_pc^2 + 2m_ec^2)^2 \approx 0.882\ \mathrm{GeV}^2, \quad (5)$$

and

$$\varepsilon_{\min} \approx m_ec^2(m_ec^2 + m_pc^2)/E. \quad (6)$$

For both processes,

$$s_{\max}(\varepsilon, E) = m_p^2c^4 + 2\varepsilon E(1+\beta) \approx m_p^2c^4 + 4\varepsilon E, \quad (7)$$

and $s_{\max}(\varepsilon, E)$ corresponds to a head-on collision of a proton of energy E and a photon of energy ε.

Examination of the integrand in Equation 1 shows that the energy of the soft photon interacting with a proton of energy E is distributed as

$$p(\varepsilon) = \frac{x_{p\gamma}(E)n(\varepsilon)}{8\beta E^2\varepsilon^2}\Phi(s_{\max}(\varepsilon, E)) \quad (8)$$

in the range $\varepsilon_{\min} \le \varepsilon \le \infty$ where

$$\Phi(s_{\max}) = \int_{s_{\min}}^{s_{\max}}\sigma(s)(s - m_p^2c^4)ds. \quad (9)$$

Similarly, examination of the integrand in Equation 1 shows that the square of the total CM frame energy is distributed as

$$p(s) = \frac{\sigma(s)(s - m_p^2c^4)}{\Phi(s_{\max})}, \quad (10)$$

in the range $s_{\min} \le s \le s_{\max}$.

The Monte Carlo rejection technique can be used to sample ε and s respectively from the two distributions, and Equation 2 is used to find θ. One then Lorentz transforms the interacting particles to the frame in which the interaction is treated (usually the proton rest frame), and samples momenta of particles produced in the interaction from the appropriate differential cross section by the rejection method. The energies of produced particles are then Lorentz transformed to the laboratory frame, and the final energy of the proton is obtained by requiring

energy conservation. In this procedure, it is not always possible to achieve exact conservation of both momentum and energy while sampling particles from inclusive differential cross sections (e.g. multiple pion production well above threshold), and the momentum of the last particle sampled is therefore adjusted to minimize the error.

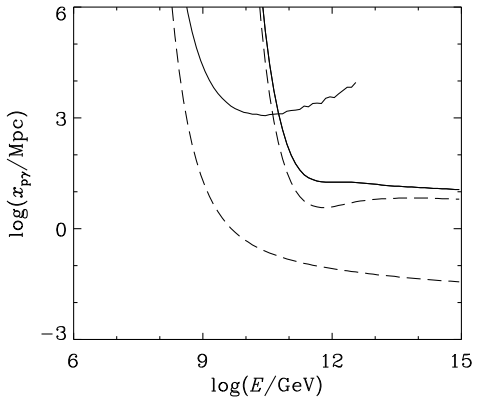

Fig. 1.— Mean interaction length (dashed lines) and energy-loss distance (solid lines), $E/(dE/dx)$, for proton-photon pair-production and pion-production in the microwave background (lower and higher energy curves respectively). (From Protheroe and Johnson 1995).

The mean interaction lengths for both processes, $x_{p\gamma}(E)$, are obtained from Equation 1 for interactions in the microwave background and are plotted as dashed lines in Fig. 1. Dividing by the inelasticity, $\kappa(E)$, one obtains the energy-loss distances for the two processes,

$$\frac{E}{dE/dx} = \frac{x_{p\gamma}(E)}{\kappa(E)}. \tag{11}$$

2.2. Nuclei

In the case of nuclei the situation is a little more complicated. The threshold condition for Bethe-Heitler pair production can be expressed as

$$\gamma > \frac{m_e c^2}{\varepsilon}\left(1 + \frac{m_e}{Am_p}\right), \tag{12}$$

and the threshold condition for pion photoproduction can be expressed as

$$\gamma > \frac{m_\pi c^2}{2\varepsilon}\left(1 + \frac{m_\pi}{2Am_p}\right). \tag{13}$$

Since $\gamma = E/Am_pc^2$, where A is the mass number, we will need to shift both energy-loss distance curves in Fig. 1 to higher energies by a factor of A. We shall also need to shift the curves up or down as discussed below.

For Bethe-Heitler pair production the energy lost by a nucleus in each collision near threshold is approximately $\Delta E \approx \gamma 2m_e c^2$. Hence the inelasticity is

$$K \equiv \frac{\Delta E}{E} \approx \frac{2m_e}{Am_p}, \tag{14}$$

and is a factor of A lower than for protons. On the other hand, the cross section goes like Z^2, so the overall shift is down (to lower energy-loss distance) by Z^2/A. For example, for iron nuclei the energy loss distance for pair production is reduced by a factor $26^2/56 \approx 12.1$.

For pion production the energy lost by a nucleus in each collision near threshold is approximately $\Delta E \approx \gamma m_\pi c^2$, and so, as for pair production, the inelasticity is factor A lower than for protons. The cross section increases approximately as $A^{0.9}$ giving an overall increase in the energy loss distance for pion production of a factor $\sim A^{0.1} \approx 1.5$ for iron nuclei. The energy loss distances for pair production and pion photoproduction are shown for iron nuclei in Fig. 2.

Photodisintegration is very important and has been considered in detail by Tkaczyk et al. (1975), Puget et al. (1976), Karakula and Tkaczyk (1993) , Epele and Roulet (1998) and Stecker and Salamon (1999). The photodisintegration distance defined by $A/(dA/dx)$ taken from Stecker and Salamon (1999) is shown in Fig. 2 together with an estimate made over a larger range of energy by Protheroe (unpublished) of the total loss distance based on photodisintegration cross sections of Karakula and Tkaczyk (1993). Since iron nuclei will be fragmented during pion photoproduction, the photodisintegration distance of Fe at high energies should be consistent with $\sim 56\times$ *the mean free path* for pion photoproduction by Fe at higher energies, and this is found to be the case (see Fig. 2).

3. Cosmic Ray Acceleration

For stochastic particle acceleration by electric fields induced by motion of magnetic fields B, the rate of energy gain by relativistic particles of charge Ze can be written (in SI units)

$$\left.\frac{dE}{dt}\right|_{\rm acc} = \xi Zec^2 B \tag{15}$$

where $\xi < 1$ and depends on the acceleration mechanism. I shall give a simple heuristic treatment of Fermi acceleration based on that given in Gaisser's excellent book (Gaisser 1990). I shall start with 2nd order Fermi

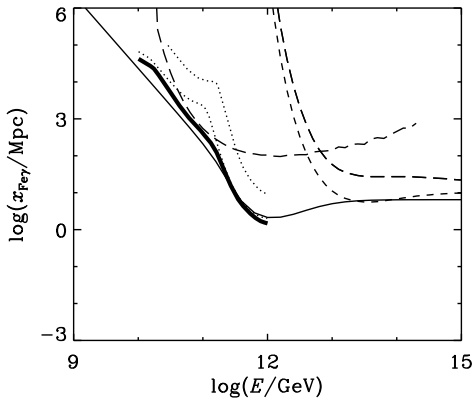

Fig. 2.— Energy-loss distance of Fe-nuclei in the CMBR for pair-production (leftmost long dashed line) and pion photoproduction (rightmost long dashed line), and mean interaction length for pion photoproduction multiplied by 56 (short dashed line) are obtained from curves in Fig. 1. The photodisintegration distances given by Stecker and Salamon (1999) for loss of one nucleon (lower dotted curve) and two nucleons (upper dotted line) are shown together with the total loss distance estimated by Stecker and Salamon (1999). The thin full curve shows an estimate over a larger range of energy (Protheroe, unpublished) of the total loss distance based on photodisintegration cross sections of Karakula and Tkaczyk (1993).

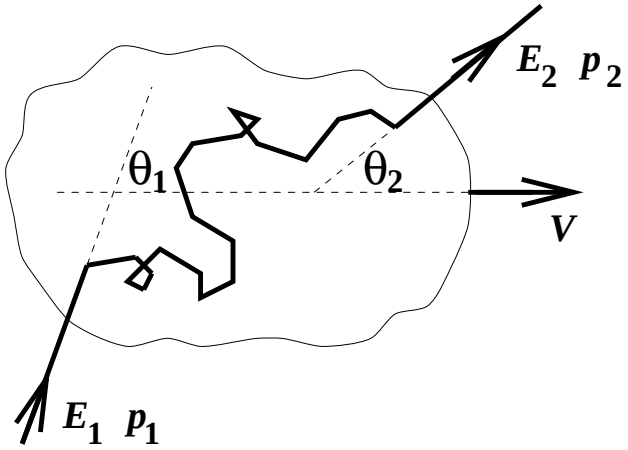

Fig. 3.— Interaction of cosmic ray of energy E_1 with "cloud" moving with speed V

acceleration (Fermi's original theory) and describe how this can be modified in the context of astrophysical shocks into the more efficient 1st order Fermi mechanism known as shock acceleration. More detailed and rigorous treatments are given in several review articles (Drury 1983a, Blandford and Eichler 1987, Berezhko and Krymsky 1988). See the review by Jones and Ellison (1991) on the plasma physics of shock acceleration which also includes a brief historical review and refers to early work.

3.1. Fermi's Original Theory

Gas clouds in the interstellar medium have random velocities of $\sim$ 15 km/s superimposed on their regular motion around the galaxy. Cosmic rays gain energy on average when scattering off these magnetized clouds. A cosmic ray enters a cloud and scatters off irregularities in the magnetic field which is tied to the cloud because it is partly ionized.

In the frame of the cloud: (a) there is no change in energy because the scattering is collisionless, and so there is elastic scattering between the cosmic ray and the cloud as a whole which is much more massive than the cosmic ray; (b) the cosmic ray's direction is randomized by the scattering and it emerges from the cloud in a random direction.

Consider a cosmic ray entering a cloud with energy E_1 and momentum p_1 travelling in a direction making angle θ_1 with the cloud's direction. After scattering inside the cloud, it emerges with energy E_2 and momentum p_2 at angle θ_2 to the cloud's direction (Fig. 3). The energy change is obtained by applying the Lorentz transformations between the laboratory frame (unprimed) and the cloud frame (primed). Transforming to the cloud frame:

$$E_1' = \gamma E_1(1 - \beta\cos\theta_1) \tag{16}$$

where $\beta = V/c$ and $\gamma = 1/\sqrt{1-\beta^2}$.
Transforming to the laboratory frame:

$$E_2 = \gamma E_2'(1 + \beta\cos\theta_2'). \tag{17}$$

The scattering is collisionless, being with the magnetic field. Since the magnetic field is tied to the cloud, and the cloud is very massive, in the cloud's rest frame there is no change in energy, $E_2' = E_1'$, and hence we obtain the fractional change in LAB-frame energy $(E_2 - E_1)/E_1$,

$$\frac{\Delta E}{E} = \frac{1 - \beta\cos\theta_1 + \beta\cos\theta_2' - \beta^2\cos\theta_1\cos\theta_2'}{1-\beta^2} - 1. \tag{18}$$

We need to obtain average values of $\cos\theta_1$ and $\cos\theta_2'$. Inside the cloud, the cosmic ray scatters off magnetic irregularities many times so that its direction is randomized,

$$\langle\cos\theta_2'\rangle = 0. \tag{19}$$

The average value of $\cos\theta_1$ depends on the rate at which cosmic rays collide with clouds at different angles. The rate of collision is proportional to the relative velocity between the cloud and the particle so that the probability per unit solid angle of having a collision at angle θ_1 is proportional to $(v - V\cos\theta_1)$. Hence, for ultrarelativistic particles ($v = c$)

$$\frac{dP}{d\Omega_1} \propto (1 - \beta\cos\theta_1), \tag{20}$$

and we obtain

$$\langle\cos\theta_1\rangle = \int \cos\theta_1 \frac{dP}{d\Omega_1} d\Omega_1 / \int \frac{dP}{d\Omega_1} d\Omega_1 = -\frac{\beta}{3}, \tag{21}$$

giving

$$\frac{\langle\Delta E\rangle}{E} = \frac{1 + \beta^2/3}{1 - \beta^2} - 1 \simeq \frac{4}{3}\beta^2 \tag{22}$$

since $\beta \ll 1$.

We see that $\langle\Delta E\rangle/E \propto \beta^2$ is positive (energy gain), but is 2nd order in β and because $\beta \ll 1$ the average energy gain is very small. This is because there are almost as many overtaking collisions (energy loss) as there are head-on collisions (energy gain).

3.2. 1st Order Fermi Acceleration at SN or Other Shocks

Fermi's original theory was modified in the 1970's (Axford, Lear and Skadron 1977, Krymsky 1977, Bell 1978, Blandford and Ostriker 1978) to describe more efficient acceleration (1st order in β) taking place at supernova shocks but is generally applicable to strong shocks in other astrophysical contexts. Our discussion of shock acceleration will be of necessity brief, and omit a number of subtleties.

Here, for simplicity, we adopt the test particle approach (neglecting effects of cosmic ray pressure on the shock profile), adopt a plane geometry and consider only non-relativistic shocks. Nevertheless, the basic concepts will be described in sufficient detail that we can consider acceleration and interactions of the highest energy cosmic rays, and to what energies they can be accelerated. We consider the classic example of a SN shock, although the discussion applies equally to other shocks. During a supernova explosion several solar masses of material are ejected at a speed of $\sim 10^4$ km/s which is much faster than the speed of sound in the interstellar medium (ISM) which is ~ 10 km/s. A strong shock wave propagates radially out as the ISM and its associated magnetic field piles up in front of the supernova ejecta. The velocity of the shock, V_S, depends on the velocity of the ejecta, V_P, and on the ratio of specific heats, γ through the compression ratio, R,

$$V_S/V_P \simeq R/(R-1). \tag{23}$$

For SN shocks the SN will have ionized the surrounding gas which will therefore be monatomic ($\gamma = 5/3$), and theory of shock hydrodynamics shows that for $\gamma = 5/3$ a strong shock will have $R = 4$.

In order to work out the energy gain per shock crossing, we can visualize magnetic irregularities on either side of the shock as clouds of magnetized plasma of Fermi's original theory (Fig. 4). By considering the rate at which cosmic rays cross the shock from downstream to upstream, and upstream to downstream, one finds $\langle\cos\theta_1\rangle = -2/3$ and $\langle\cos\theta_2'\rangle = 2/3$, giving

$$\frac{\langle\Delta E\rangle}{E} \simeq \frac{4}{3}\beta \simeq \frac{4}{3}\frac{V_P}{c} \simeq \frac{4}{3}\frac{(R-1)}{R}\frac{V_S}{c}. \tag{24}$$

Note this is 1st order in $\beta = V_P/c$ and is therefore more efficient than Fermi's original theory. This is because of the converging flow – whichever side of the shock you are on, if you are moving with the plasma, the plasma on the other side of the shock is approaching you at speed V_p.

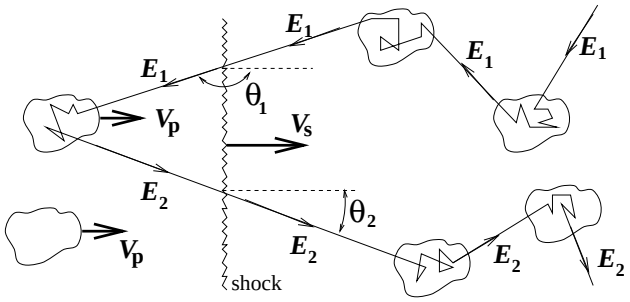

Fig. 4.— Interaction of cosmic ray of energy E_1 with a shock moving with speed V_s.

To obtain the energy spectrum we need to find the probability of a cosmic ray encountering the shock once, twice, three times, etc. If we look at the diffusion of a cosmic ray as seen in the rest frame of the shock (Fig. 5), there is clearly a net flow of the energetic particle population in the downstream direction.

The net flow rate downstream gives the rate at which cosmic rays are lost downstream

$$r_{\rm loss} = n_{\rm CR} V_S/R \qquad {\rm m}^{-2}{\rm s}^{-1} \tag{25}$$

since cosmic rays with number density $n_{\rm CR}$ at the shock are advected downstream with speed V_S/R (from right to left in Fig. 5) and we have neglected relativistic transformations of the rates because $V_S \ll c$.

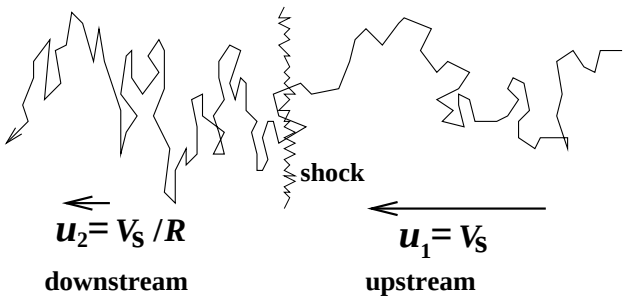

Fig. 5.— Diffusion of cosmic rays from upstream to downstream seen in the shock frame speed V_s.

Upstream of the shock, cosmic rays travelling at speed v at angle θ to the shock normal (as seen in the laboratory frame) approach the shock with speed $(V_S + v\cos\theta)$ as seen in the shock frame. Clearly, to cross the shock, $\cos\theta > -V_S/v$. Then, assuming cosmic rays upstream are isotropic, the rate at which they cross from upstream to downstream is

$$\begin{aligned} r_{\rm cross} &= n_{\rm CR}\frac{1}{4\pi}\int_{-V_S/v}^{1}(V_S + v\cos\theta)2\pi d(\cos\theta) \\ &\approx n_{\rm CR}v/4 \quad {\rm m}^{-2}{\rm s}^{-1}. \end{aligned} \tag{26}$$

The probability of crossing the shock once and then escaping from the shock (being lost downstream) is the ratio of these two rates:

$${\rm Prob.(escape)} = r_{\rm loss}/r_{\rm cross} \approx 4V_S/Rv. \tag{27}$$

The probability of returning to the shock after crossing from upstream to downstream is

$${\rm Prob.(return)} = 1 - {\rm Prob.(escape)}, \tag{28}$$

and so the probability of returning to the shock k times and also of crossing the shock at least k times is

$${\rm Prob.(cross} \geq k) = [1 - {\rm Prob.(escape)}]^k. \tag{29}$$

Hence, the energy after k shock crossings is

$$E = E_0\left(1 + \frac{\Delta E}{E}\right)^k \tag{30}$$

where E_0 is the initial energy.

To derive the spectrum, we note that the integral energy spectrum (number of particles with energy greater than E) on acceleration must be

$$Q(>E) \propto [1 - {\rm Prob.(escape)}]^k \tag{31}$$

where

$$k = \frac{\ln(E/E_0)}{\ln(1 + \Delta E/E)}. \tag{32}$$

Hence,

$$\ln Q(>E) = A + \frac{\ln(E/E_0)}{\ln(1 + \Delta E/E)}\ln[1 - {\rm Prob.(escape)}], \tag{33}$$

where A is a constant, and so

$$\ln Q(>E) = B - (\Gamma - 1)\ln E \tag{34}$$

where B is a constant and

$$\Gamma = 1 - \frac{\ln[1 - {\rm Prob.(escape)}]}{\ln(1 + \Delta E/E)} \approx \frac{R+2}{R-1}. \tag{35}$$

Hence we arrive at the spectrum of cosmic rays on acceleration

$$Q(>E) \propto E^{-(\Gamma-1)} \qquad \text{(integral form)} \tag{36}$$

$$Q(E) \propto E^{-\Gamma} \qquad \text{(differential form)}. \tag{37}$$

For $R = 4$ we have the well-known E^{-2} differential spectrum. The observed cosmic ray spectrum is steepened by energy-dependent escape of cosmic rays from the Galaxy.

3.3. Effect of cosmic ray pressure

For simplicity, we have neglected the effect of cosmic ray pressure on the shock which can alter the shock profile. The original method of treating this non-linear effect is the two-fluid method, the two-fluids being plasma and cosmic rays, and this is reviewed by Drury (1983b). The shock profile, instead of being a step-function becomes smoothed, and this affects the acceleration of low and high energy particles differently. Lower energy particles with short diffusion mean free paths spanning only part of the shock profile (i.e. effectively seeing a lower R) will have a steeper spectrum, while high energy particles with longer diffusion mean free paths spanning most of the shock profile (i.e. effectively seeing a higher R) will have a flatter spectrum. The net result of this is a spectrum with upward curvature. In addition, as a result of the cosmic ray pressure far downstream providing additional slowing of the plasma, the overall compression ratio from far upstream to far downstream may be even higher than in the test particle case giving an even flatter spectrum for the highest energy particles (Ellison and Eichler 1984; see Baring 1997 for a brief review and additional references).

3.4. Relativistic Shocks

Shocks in jets of active galactic nuclei (AGN) and gamma ray bursts (GRB) are likely to be relativistic, i.e. $u_1 > 0.1c$. This will affect the acceleration in two ways: (a) the adiabatic index of a relativistic gas is $\gamma = 4/3$ giving $R = 7$ for a strong shock, and so one would expect from Eq. 35 a flatter spectrum with $\Gamma = 1.5$. However, for relativistic plasma motion with bulk velocities comparable to those of the particles being accelerated, the approximations used to derive Eqns. 25 and 26 are no longer valid, the escape probability being greater and the particles being anisotropic, with the result that $\Gamma > 1.5$. Detailed studies have shown a trend in which shocks with larger u_1 generally have lower Γ (Kirk and Schneider 1987, Ellison and Jones 1990). However, the spectral index is very sensitive to the pitch angle (see Baring 1997 for additional references).

4. Shock Acceleration Rate

Here we again neglect effects of cosmic ray pressure and consider only a non-relativistic shock. The acceleration rate is defined by

$$r_{\rm acc} \equiv \frac{1}{E}\left.\frac{dE}{dt}\right|_{\rm acc} = \frac{(\langle \Delta E\rangle/E)}{t_{\rm cycle}} \approx \frac{4}{3}\frac{(R-1)}{R}\frac{V_S}{c}t_{\rm cycle}^{-1} \tag{38}$$

where $t_{\rm cycle}$ is the time for one complete cycle, i.e. from crossing the shock from upstream to downstream, diffusing back towards the shock and crossing from downstream to upstream, and finally returning to the shock.

The rate of loss of accelerated particles downstream is the probability of escape per shock crossing divided by the cycle time

$$r_{\rm esc} = \frac{\rm Prob.(escape)}{t_{\rm cycle}} \approx \frac{4}{R}\frac{V_S}{c}t_{\rm cycle}^{-1} \tag{39}$$

We see immediately that the ratio of the escape rate to the acceleration rate depends on the compression ratio

$$\frac{r_{\rm esc}}{r_{\rm acc}} \approx \frac{3}{R-1} \tag{40}$$

and for a strong shock ($R = 4$) the two rates are equal. As we shall see later, a consequence of this is that the asymptotic spectrum of particles accelerated by a strong shock is the well-known E^{-2} power-law.

We shall discuss these processes in the shock frame (see Fig. 5) and consider first particles crossing the shock from upstream to downstream and diffusing back to the shock, i.e. we shall work out the average time spent downstream. Since we are considering non-relativistic shocks, the time scales are approximately the same in the upstream and downstream plasma frames, and so in this section I shall drop the use of subscripts indicating the frame of reference.

Diffusion takes place in the presence of advection at speed u_2 in the downstream direction. The typical distance a particle diffuses in time t is $\sqrt{k_2 t}$ where k_2 is the diffusion coefficient in the downstream region. The distance advected in this time is simply $u_2 t$. If $\sqrt{k_2 t} \gg u_2 t$ the particle has a very high probability of returning to the shock, and if $\sqrt{k_2 t} \ll u_2 t$ the particle has a very high probability of never returning to the shock (i.e. it has effectively escaped downstream). So, we set $\sqrt{k_2 t} = u_2 t$ to define a distance k_2/u_2 downstream of the shock which is effectively a boundary between the region closer to the shock where the particles will usually return to the shock and the region farther from the shock in which the particles will usually be advected downstream never to return. There are $n_{\rm CR}k_2/u_2$ particles per unit area of shock between the shock and this boundary. Dividing this by $r_{\rm cross}$ we obtain the average time spent downstream before returning to the shock

$$t_2 \approx \frac{4}{c}\frac{k_2}{u_2}. \tag{41}$$

Consider next the other half of the cycle after the particle has crossed the shock from downstream to upstream until it returns to the shock. In this case we can define a boundary at a distance k_1/u_1 upstream of the shock such that nearly all particles upstream of this boundary have never encountered the shock, and nearly all the particles between this boundary and the shock have diffused there from the shock. Then dividing the number of particles per unit area of shock between the shock and this boundary, $n_{\rm CR}k_1/u_1$, by $r_{\rm cross}$ we obtain the average time spent upstream before returning to the shock

$$t_1 \approx \frac{4}{c}\frac{k_1}{u_1}, \tag{42}$$

and hence the cycle time

$$t_{\rm cycle} \approx \frac{4}{c}\left(\frac{k_1}{u_1} + \frac{k_2}{u_2}\right). \tag{43}$$

The acceleration rate is then given by

$$r_{\rm acc} \approx \frac{(R-1)u_1}{3R}\left(\frac{k_1}{u_1} + \frac{k_2}{u_2}\right)^{-1}. \tag{44}$$

Assuming that the diffusion coefficients upstream and downstream have the same power-law dependence on energy, e.g.,

$$k_1 \propto k_2 \propto E^{\delta}, \tag{45}$$

then the acceleration rate also has a power-law dependence

$$r_{\rm acc} \propto E^{-\delta}. \quad (46)$$

Note that more correctly, the diffusion coefficient will be a function of magnetic rigidity, ρ, which, for ultra-relativistic particles considered in this paper, is approximately equal to E/Ze where Ze is the charge. However, here we are mainly concerned with singly charged particles and shall work in terms of E rather than rigidity.

4.1. Maximum acceleration rate

We next consider the diffusion for the cases of parallel, oblique, and perpendicular shocks, and estimate the maximum acceleration rate for these cases. The diffusion coefficients required, k_1 and k_2, are the coefficients for diffusion parallel to the shock normal. The diffusion coefficient along the magnetic field direction is some factor η times the minimum diffusion coefficient, known as the Bohm diffusion coefficient,

$$k_\parallel = \eta \frac{1}{3} r_g c \quad (47)$$

where r_g is the gyroradius, and $\eta > 1$.

Parallel shocks are defined such that the shock normal is parallel to the magnetic field ($\vec{B} || \vec{u_1}$). In this case, making the approximation that $k_1 = k_2 = k_\parallel$ and $B_1 = B_2$ one obtains

$$t^\parallel_{\rm acc} \approx \frac{20}{3} \frac{\eta E}{eB_1 u_1^2}. \quad (48)$$

For a shock speed of $u_1 = 0.1c$ and $\eta = 10$ one obtains an acceleration rate (in SI units) of

$$\left.\frac{dE}{dt}\right|_{\rm acc} \approx 1.5 \times 10^{-4} ec^2 B. \quad (49)$$

For the oblique case, the angle between the magnetic field direction and the shock normal is different in the upstream and downstream regions, and the direction of the plasma flow also changes at the shock. The diffusion coefficient in the direction at angle θ to the magnetic field direction is given by

$$k = k_\parallel \cos^2\theta + k_\perp \sin^2\theta \quad (50)$$

where $k_\perp$ is the diffusion coefficient perpendicular to the magnetic field. Jokipii (1987) shows that

$$k_\perp \approx \frac{k_\parallel}{1+\eta^2} \quad (51)$$

provided that η is not too large (values in the range up to 10 appear appropriate), and that acceleration at perpendicular shocks can be much faster than for the parallel case. For $k_{xx} = k_\perp$ and $B_2 \approx 4B_1$ and one obtains

$$t^\perp_{\rm acc} \approx \frac{8}{3} \frac{E}{\eta e B_1 u_1^2}. \quad (52)$$

For a shock speed of $u_1 = 0.1c$ and $\eta = 10$ one obtains an acceleration rate (in SI units) of

$$\left.\frac{dE}{dt}\right|_{\rm acc} \approx 0.04 ec^2 B. \quad (53)$$

Supernova shocks remain strong enough to continue accelerating cosmic rays for about 1000 years. The rate at which cosmic rays are accelerated is inversely proportional to the diffusion coefficient (faster diffusion means less time near the shock). For the maximum feasible acceleration rate, a typical interstellar magnetic field, and 1000 years for acceleration, energies of $10^{14} \times Z$ eV are possible (Z is atomic number) at parallel shocks and $10^{16} \times Z$ eV at perpendicular shocks.

In the case of acceleration by relativistic shocks (e.g. Bednarz & Ostrowski 1996, 1998, and Bednarz 1998, and Ostrowski 1998), the acceleration time depends strongly on u_1, $k_\perp/k_\parallel$, and θ and can be as low as $\sim (1—10) r_g/c$.

5. Maximum Energies

Protons and nuclei can be accelerated to much higher energies than electrons for a given magnetic environment. For stochastic particle acceleration by electric fields induced by motion of magnetic fields B, the rate of energy gain by relativistic particles of charge Ze can be written (in SI units) $dE/dt = \xi Z e c^2 B$ as in Eq. 1, where $\xi < 1$ and depends on the acceleration mechanism; a value of $\xi = 0.04$ might be achieved by first order Fermi acceleration at a perpendicular shock with shock speed $\sim 0.1c$.

5.1. Limits from Synchrotron Losses

The rate of energy loss by synchrotron radiation of a particle of mass Am_p, charge Ze, and energy γmc^2 is

$$-\left.\frac{dE}{dt}\right|_{\rm syn} = \frac{4}{3}\sigma_T \left(\frac{Z^2 m_e}{A m_p}\right)^2 \frac{B^2}{2\mu_0} \gamma^2 c. \quad (54)$$

Equating the rate of energy gain with the rate of energy loss by synchrotron radiation places one limit on the maximum energy achievable by electrons, protons and nuclei:

$$E_e^{\rm max} = 6.0 \times 10^2 \xi^{1/2} \left(\frac{B}{1\ {\rm T}}\right)^{-1/2} \ {\rm GeV}, \quad (55)$$

$$E_p^{\max} = 2.0 \times 10^9 \xi^{1/2} \left(\frac{B}{1\,\mathrm{T}}\right)^{-1/2} \quad \mathrm{GeV}, \quad (56)$$

$$E_{Z,A}^{\max} = 2.0 \times 10^9 \xi^{1/2} \frac{A^2}{Z^{3/2}} \left(\frac{B}{1\,\mathrm{T}}\right)^{-1/2} \mathrm{GeV}. \quad (57)$$

The cut-off in proton spectrum may be caused by synchrotron radiation, and Totani (1998) has found that synchrotron radiation by highest energy protons could account for much of the observed cosmic γ-ray background. The maximum energies of protons and iron nuclei allowed by synchrotron radiation losses are shown in Figs. 6 and 7 respectively, and are plotted against magnetic field for three values of ξ. The straight lines are for: the maximum possible acceleration rate $\xi = 1$ (dashed), plausible acceleration at perpendicular shock $\xi = 0.04$ (solid), and plausible acceleration at parallel shock $\xi = 1.5 \times 10^{-4}$ (dot-dash).

Other limits on the maximum energy are placed by the dimensions of the acceleration region and the time available for acceleration. These limits were obtained and discussed in some detail by Biermann and Strittmatter (1987).

5.2. Limits from Interactions with Radiation

Equating the total energy loss rate for proton–photon interactions (i.e. the sum of pion production and Bethe-Heitler pair production) in Fig. 1 to the rate of energy gain by acceleration gives the maximum proton energy in the absence of other loss processes. This is shown in Fig. 6 as a function of magnetic field which determines the rate of energy gain through Eq. 15. The result is shown by the curves for the maximum possible acceleration rate $\xi = 1$ (dashed), plausible acceleration at perpendicular shock $\xi = 0.04$ (solid), and plausible acceleration at parallel shock $\xi = 1.5 \times 10^{-4}$ (dot-dash). Also shown is the maximum energy determined by synchrotron losses (thick lines) for the three cases. As can be seen, for a perpendicular shock it is possible to accelerate protons to $\sim 10^{13}$ GeV in a $\sim 10^{-5}$ G field.

The effective loss distance given in Fig. 2 is used together with the acceleration rate for iron nuclei to obtain the maximum energy as a function of magnetic field. This is shown in Fig. 7 which is analogous to Fig. 6 for protons. We see that for a perpendicular shock it is possible to accelerate iron nuclei to $\sim 2\times10^{14}$ GeV in a $\sim 3\times10^{-5}$ G field. While this is higher than for protons, iron nuclei are likely to get photodisintegrated into nucleons of maximum energy $\sim 4 \times 10^{12}$ GeV, and so there is not much to be gained unless the source is nearby. Of course, potential acceleration sites need to have the appropriate combination of size (much larger than the gyroradius at the maximum energy), magnetic field, and shock velocity (or other relevant velocity), and these criteria have been discussed in detail by Hillas (1984).

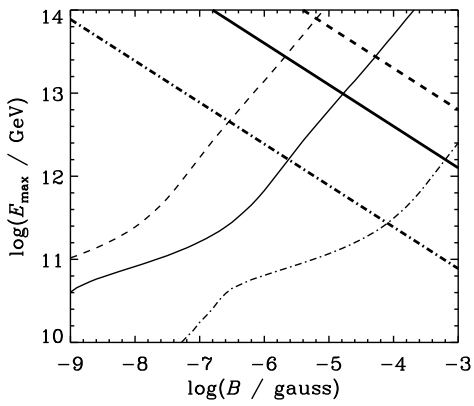

Fig. 6.— Maximum proton energy as a function of magnetic field. Straight lines give the limit from synchrotron loss, curved lines give the limit from pion photoproduction. $E_{\max}$ is given for $\xi = 1$ (dashed), $\xi = 0.04$ (solid), $\xi = 1.5 \times 10^{-4}$ (dot-dash).

6. Spectral Shape near Maximum Energy

To determine the spectral shape near maximum energy we use the leaky-box acceleration model (Szabo and Protheroe 1994) which may be considered as follows. A particle of energy E_0 is injected into the leaky box. While inside the box, the particle's energy changes at a rate $dE/dt = Er_{\rm acc}(E)$ and that in any short time interval Δt the particle has a probability of escaping from the box given by $\Delta t r_{\rm esc}(E)$. The energy spectrum of particles escaping from the box then approximates the spectrum of shock accelerated particles.

Let us consider first the case of no energy losses, interactions, or losses due to any other process. N_0 particles of energy E_0 are injected at time $t = 0$, and we assume the following acceleration and escape rates:

$$r_{\rm acc} = aE^{-\delta}, \quad (58)$$

$$r_{\rm esc} = cE^{-\delta}. \quad (59)$$

The energy at time t is then obtained simply by integrating

$$dE/dt = aE^{(1-\delta)}, \quad (60)$$

giving

$$E(t) = (E_0^\delta + \delta a t)^{1/\delta}. \quad (61)$$

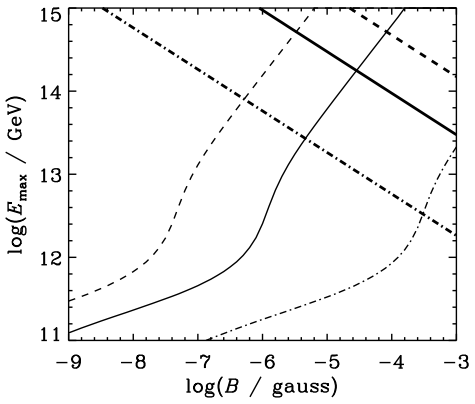

Fig. 7.— Maximum iron nucleus energy as a function of magnetic field. Straight lines give the limit from synchrotron loss, curved lines give the limit from photodisintegration. $E_{\rm max}$ is given for $\xi = 1$ (dashed), $\xi = 0.04$ (solid), $\xi = 1.5 \times 10^{-4}$ (dot-dash).

The number of particles remaining inside the accelerator at time t after injection is obtained by solving

$$dN/dt = -N(t)c[E(t)]^{-\delta}. \quad (62)$$

Using Eq. 61 and integrating, one has

$$\int_{N_0}^{N(t)} N^{-1}dN = -c\int_0^t (E_0^\delta + \delta a t)^{-1}dt, \quad (63)$$

giving

$$N(t) = N_0[E(t)/E_0]^{-c/a}. \quad (64)$$

Since $N_0 - N(t)$ particles have escaped from the accelerator before time t, and therefore have energies between E_0 and $E(t)$, the differential energy spectrum of particles which have escaped from the accelerator is simply given by

$$dN/dE = N_0(\Gamma-1)(E_0)^{-1}(E/E_0)^{-\Gamma}, \quad (65)$$

for $(E > E_0)$ where $\Gamma = (1 + c/a)$ is the differential spectral index. We note that for $r_{\rm esc}(E) = r_{\rm acc}(E)$ one obtains the standard result for acceleration at strong shocks $\Gamma = 2$.

6.1. Cut-off due to finite acceleration volume, etc.

Even in the absence of energy losses, acceleration usually ceases at some energy due to the finite size of the acceleration volume (e.g. when the gyroradius becomes comparable to the characteristic size of the shock), or as a result of some other process. We approximate the effect of this by introducing a constant term to the expression for the escape rate:

$$r_{\rm esc} = cE^{-\delta} + cE_{\rm max}^{-\delta}. \quad (66)$$

where $E_{\rm max}$ is defined by the above equation and will be close to the energy at which the spectrum steepens due to the constant escape term. We shall refer to $E_{\rm max}$ as the "maximum energy" even though some particles will be accelerated to energies above this.

Following the same procedure as for the case of a purely power-law dependence of the escape rate, we obtain the differential energy spectrum of particles ($E > E_0$) escaping from the accelerator,

$$\frac{dN}{dE} = N_0(\Gamma-1)(E_0)^{-1}(E/E_0)^{-\Gamma}[1+(E/E_{\rm max})^\delta] \times \exp\left\{-\frac{\Gamma-1}{\delta}\left[\left(\frac{E}{E_{\rm max}}\right)^\delta - \left(\frac{E_0}{E_{\rm max}}\right)^\delta\right]\right\} \quad (67)$$

for $\delta > 0$. For $\delta = 0$ we note that from Eq. 66 $r_{\rm esc} = (2c)$ at all energies. Thus the situation is equivalent to the case of $E_{\rm max} \to \infty$ and the spectrum is given by Eq. 65 provided we replace c with $2c$, i.e. we must replace Γ with $\Gamma' = (2\Gamma - 1)$. We compare in Fig 8 the spectra for $\Gamma = 2$ and δ ranging from 1/3 to 1, and note that the energy dependence of the diffusion coefficient has a profound influence on the shape of the cut-off.

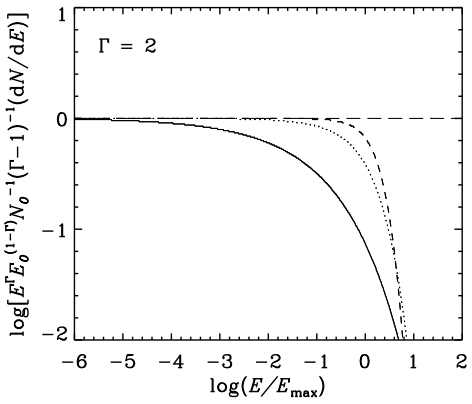

Fig. 8.— Differential energy spectrum for $\Gamma = 2$ and $\delta = 1/3$ (solid curve), 2/3 (dotted curve) and 1 (dashed curve). (From Protheroe & Stanev 1998).

Spectra such as those presented in Fig. 8 may be used to model the source spectra of high energy cosmic ray nuclei of various species if one replaces energy with magnetic rigidity, $\rho = pc/Ze \approx E/Ze$, where Z is the atomic number:

$$\frac{dN}{d\rho} = N_0(\Gamma-1)(\rho_0)^{-1}(\rho/\rho_0)^{-\Gamma}[1+(\rho/\rho_{\rm max})^{\delta}] \times \exp\left\{-\frac{\Gamma-1}{\delta}\left[\left(\frac{\rho}{\rho_{\rm max}}\right)^{\delta}-\left(\frac{\rho_0}{\rho_{\rm max}}\right)^{\delta}\right]\right\} \quad (68)$$

for $\rho > \rho_0$.

6.2. Cut-off due to E^2 energy losses

E^2 energy losses of protons or nuclei at extremely high energies result from synchrotron radiation. The introduction of continuous energy losses into the problem is, in principle, straightforward and accomplished simply by modifying Eq. 60,

$$dE/dt = aE^{(1-\delta)} - bE^2. \quad (69)$$

Setting $dE/dt = 0$ we obtain the cut-off energy

$$E_{\rm cut} = (a/b)^{1/(1+\delta)}. \quad (70)$$

For this case, however, the problem is easier to solve using the Green's function approach adopted by Stecker (1971) when considering the ambient spectrum of cosmic ray electrons and galactic γ-rays. Using the appropriate Green's function one can obtain the steady-state spectrum of particles inside the leaky-box accelerator, and multiplying this by the escape rate one obtains the spectrum of particles leaving the accelerator,

$$\frac{dN}{dE} = \frac{c\,E^{-\delta}+E_{\rm max}^{-\delta}}{a\,E^{1-\delta}-b\,E^2}\exp[-I(E)] \quad (71)$$

where

$$I(E) \equiv \int_{E_0}^{E}\frac{c\,E^{-\delta}+E_{\rm max}^{-\delta}}{a\,E^{1-\delta}-b\,E^2}\,dE \quad (72)$$

$$= \left[\left(\frac{c}{a\,\delta}\right)\left(\frac{E}{E_{\rm max}}\right)^{\delta} \times {}_2F_1\left(\frac{\delta}{1+\delta},1,1+\frac{\delta}{1+\delta},\frac{b\,E^{1+\delta}}{a}\right) - \frac{c}{a(1+\delta)}\ln\left(b-\frac{a}{E^{1+\delta}}\right)\right]_{E_0}^{E}, \quad (73)$$

and ${}_2F_1$ is the hypergeometric function.

The result depends on the parameters δ, Γ, E_0, $E_{\rm cut}$, $E_{\rm max}$. As a result of the energy loss by particles near the maximum energy a pile-up in the spectrum may be produced just below $E_{\rm cut}$. The size of the pile-up will be determined by the relative importance of $r_{\rm acc}$ and $r_{\rm esc}$ at energies just below $E_{\rm cut}$, and so should depend only on Γ and δ provided $E_0 \ll E_{\rm cut} \ll E_{\rm max}$. In this case, the shape of the spectrum is given by

$$\frac{dN}{dE} = N_0(\Gamma-1)(E_0)^{-1}\left(\frac{E}{E_0}\right)^{-\Gamma} \times \left[1-\left(\frac{E}{E_{\rm cut}}\right)^{(1+\delta)}\right]^{(\Gamma-2-\delta)/(1+\delta)}. \quad (74)$$

We compare in Fig. 9 the spectra for this case for $\delta = 1/3$, 2/3 and 1, and for $\Gamma = 1.5$, 2, and 2.5, and note that the pile-ups are higher for flatter spectra, and that for steep spectra the pile-up may be absent or the spectrum may steepen before the cut-off if δ is small. The effect of synchrotron losses on multiple diffusive shock acceleration have been considered by Melrose and Crouch (1997) , and similar effects were found.

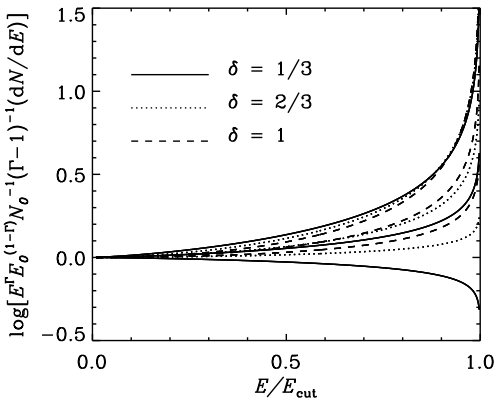

Fig. 9.— Differential energy spectra for $E_0 \ll E_{\rm cut} \ll E_{\rm max}$ for $\delta = 1/3$ (solid curves), 2/3 (dotted curves) and 1 (dashed curves), and $\Gamma = 1.5$ (upper curves), 2.0 (middle curves) and 2.5 (lower curves). (From Protheroe & Stanev 1998).

6.3. Cut-off due to pion photoproduction

Here I discuss how one can use the Monte Carlo method to investigate the shape of the cut-off or pile-up which results when the nominal cut-off energy is determined by interactions rather than continuous energy losses. This technique was used by Protheroe and Stanev

(1998) to investigate cut-offs in electron spectra due to inverse Compton scattering in the Klein-Nishina regime, and by Szabo and Protheroe(1994) to investigate cut-offs in the proton spectrum due to photoproduction in a radiation field.

The technique uses the leaky-box acceleration model described above. We describe here the case considered by Szabo and Protheroe: $\Gamma = 2, \delta = 1$. Particles of energy E_0 are injected and accelerated at a constant rate $a = \mathrm{d}E/\mathrm{d}t$. The time scale for escape from the leaky box is equal to the acceleration time scale, $t_{\rm esc} = t_{\rm acc} = E/a$, and so the probability of reaching an energy E without escaping is $P_{\rm surv}(E) = E_0/E$. Such a model produces an E^{-2} spectrum at energies above E_0 and may be easily adapted to calculations in which other processes take place in addition to acceleration, and are simulated by the Monte Carlo method.

To calculate the spectrum of particles produced during acceleration per injected particle, we use a method of weights. If a particle is injected with energy E_0, then the "weight" of the particle by the time it reaches an energy E_1 is set to the probability of it not having escaped, $W_1 = E_0/E_1$. If the particle interacts, and has energy E_1' after the interaction, etc., then the weight of the particle at the nth interaction is given by

$$W_n = \frac{E_0}{E_1}\frac{E_1'}{E_2}\cdots\frac{E_{n-1}'}{E_n}. \qquad (75)$$

For the case in which $E_{\rm max}$ is determined by proton-photon collisions, the following procedure was adopted. (i) Inject a particle with energy E_0 into the accelerator and after $(n-1)$ interactions (assuming it has survived catastrophic losses) it will have energy E_{n-1}' and weight W_{n-1}; (ii) Sample the nth path length for two competing interactions, the competing interaction with the shortest path length being assumed to be the one that occurs.

Before the interaction, the proton has energy E_n and the interaction is modelled by the Monte Carlo method. The energies of the produced particles are binned in energy with the appropriate weight, in this case W_n. The 'fraction' of the particle which does not interact, in this case $(1 - W_n)$, is assumed to escape from the accelerator and have an E^{-2} energy distribution over the energy range E_{n-1}' to E_n. This contribution is then added to the escaping proton spectrum. The process is repeated until the particle suffers a catastrophic loss in the form of a pion photoproduction reaction in which a neutron is produced.

In this way one can calculate the spectra of protons, neutrons, pions (neutral and charged) and electrons (including positrons) produced during acceleration. Results for $E_{\rm cut} = 2 \times 10^{12}$ GeV due to photoproduction on the cosmic microwave background radiation are shown in Figure 10.

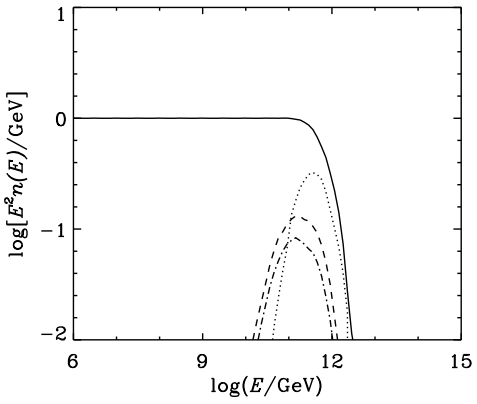

Fig. 10.— The spectrum of particles produced during acceleration (multiplied by E^2) per proton injected into the accelerator: protons (full curve), neutrons (dotted curve), charged pions (dashed curve) and neutral pions. Results are shown for $E_{\rm cut} = 2 \times 10^{12}$ GeV due to photoproduction on the cosmic microwave background. (Adapted from Fig. 7 of Szabo and Protheroe 1994).

7. Cascading During Propagation

As well as particles being produced during the acceleration process as a result of interactions, during propagation to Earth cascading occurs and the accompanying fluxes of γ-rays and neutrinos must not exceed the observed flux or flux limits. Waxman and Bahcall (1998) estimate the maximum allowed neutrino flux to be very low and model independent in the important TeV to PeV range. However, Mannheim et al. (1998) obtain a limit in this energy range which is orders of magnitude higher. By measuring the accompanying fluxes, we may well provide additional clues to the nature and origin of the highest energy cosmic rays. Hence it is important to calculate these fluxes resulting from cascading.

There are several cascade processes which are important for UHE cosmic rays propagating over large distances through a radiation field: protons interact with photons resulting in pion production and pair production; electrons interact via inverse-Compton scattering and triplet pair production, and emit synchrotron radiation in the intergalactic magnetic field; γ-rays interact by pair production. Energy losses due to cosmological redshifting of high energy particles and γ-rays can also be important, and the cosmological redshifting of the back-

ground radiation fields means that energy thresholds and interaction lengths for the above processes also change with epoch (see e.g. Protheroe et al. (1995)).

The energy density of the extragalactic background radiation is dominated by that from the cosmic microwave background at a temperature of 2.73 K. Other components of the extragalactic background radiation are discussed in the review of Ressel and Turner (1990). The extragalactic radiation fields important for cascades initiated by UHE cosmic rays include the cosmic microwave background, the radio background and the infrared–optical background. The radio background was measured over twenty years ago (Bridle 1967, Clarke et al. 1970), but the fraction of this radio background which is truly extragalactic, and not contamination from our own Galaxy, is still debatable. Berezinsky (1969) was first to calculate the mean free path on the radio background. More recently Protheroe and Biermann (1996) have made a new calculation of the extragalactic radio background radiation down to kHz frequencies. The main contribution to the background is from normal galaxies and is uncertain due to uncertainties in their evolution. The mean free path of photons in this radiation field as well as in the microwave and infrared backgrounds is shown in Fig. 11. Also shown is the mean interaction length for muon pair-production which is negligible in comparison with interactions with pair production on the radio background and double pair production on the microwave background.

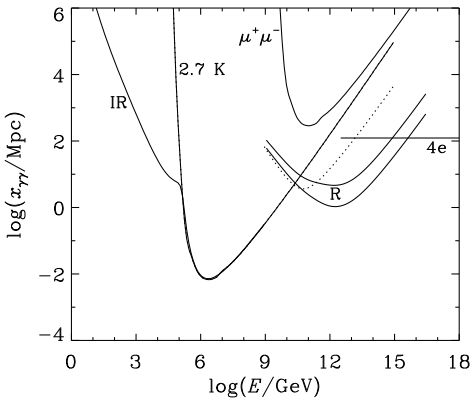

Fig. 11.— The mean interaction length for pair production for γ-rays in the Radio Background calculated in the present work (solid curves labelled R: upper curve – no evolution of normal galaxies; lower curve – pure luminosity evolution of normal galaxies) and in the radio background of Clark (1970) (dotted line). Also shown are the mean interaction length for pair production in the microwave background (2.7K), the infrared and optical background (IR), and muon pair production ($\mu^+\mu^-$) and double pair production (4e) in the microwave background (Protheroe and Johnson 1995). (From Protheroe and Biermann 1996).

Inverse Compton interactions of high energy electrons and triplet pair production can be modelled by the Monte Carlo technique (e.g. Protheroe 1986, Protheroe 1990, Protheroe et al. 1992, Mastichiadis et al. 1994), and the mean interaction lengths and energy-loss distances for these processes are given in Fig. 12. Synchrotron losses must also be included in calculations and the energy-loss distance has been added to Fig. 12 for various magnetic fields.

7.1. Practical Aspects of the Cascade

Where possible, to take account of the exact energy dependences of cross-sections, one can use the Monte Carlo method. However, direct application of Monte Carlo techniques to cascades dominated by the physical processes described above over cosmological distances takes excessive computing time. Another approach based on the matrix multiplication method has been described by Protheroe (1986) and developed in later papers (Protheroe and Stanev 1993, Protheroe and Johnson 1995). A Monte Carlo program is used to calculate the yields of secondary particles due to interactions with radiation, and spectra of produced pions are decayed (e.g. using routines in SIBYLL (Fletcher et al. 1994)) to give yields of γ-rays, electrons and neutrinos. For the pion photoproduction interactions a new program called SOPHIA is available (Mücke et al. 1998). The yields are then used to build up transfer matrices which describe the change in the spectra of particles produced after propagating through the radiation fields for a distance δx. Manipulation of the transfer matrices as described below enables one to calculate the spectra of particles resulting from propagation over arbitrarily large distances.

7.2. Matrix Method

In the work of Protheroe and Johnson (1995), fixed logarithmic energy bins were used, and the energy spectra of particles of type α ($\alpha = \gamma, e, p, n, \nu_e, \bar{\nu}_e, \nu_\mu, \bar{\nu}_\mu$) at distance x in the cascade are represented by vectors $F_j^\alpha(x)$ which give the total number of particles of type α in the jth energy bin at distance x. Transfer matrices, $\mathrm{T}_{ij}^{\alpha\beta}(\delta x)$, give the number of particles of type β in the bin j which result at a distance δx after a particle of type α and energy in bin i initiates a cascade. Then, given the spectra of particles at distance x one can obtain the

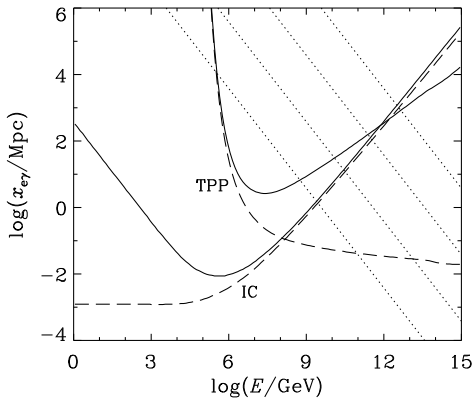

Fig. 12.— The mean interaction length (dashed line) and energy-loss distance (solid line), $E/(dE/dx)$, for electron-photon triplet pair production (TPP) and inverse-Compton scattering (IC) in the microwave background. The energy-loss distance for synchrotron radiation is also shown (dotted lines) for intergalactic magnetic fields of 10^{-9} (bottom), 10^{-10}, 10^{-11}, and 10^{-12} gauss (top). (From Protheroe and Johnson 1995.)

spectra at distance $(x + \delta x)$

$$F_j^\beta(x+\delta x) = \sum_\alpha \sum_{i=j}^{180} \mathrm{T}_{ij}^{\alpha\beta}(\delta x) F_i^\alpha(x) \qquad (76)$$

where $F_i^\alpha(x)$ are the input spectra (number in the ith energy bin) of species α.

We could also write this as

$$[\mathrm{F}(x+\delta x)] = [\mathrm{T}(\delta x)][\mathrm{F}(x)] \qquad (77)$$

where

$$[\mathrm{F}] = \begin{bmatrix} F^\gamma \\ F^e \\ F^p \\ \vdots \end{bmatrix}, \quad [\mathrm{T}] = \begin{bmatrix} \mathrm{T}^{\gamma\gamma} & \mathrm{T}^{e\gamma} & \mathrm{T}^{p\gamma} & \cdots \\ \mathrm{T}^{\gamma e} & \mathrm{T}^{ee} & \mathrm{T}^{pe} & \cdots \\ \mathrm{T}^{\gamma p} & \mathrm{T}^{ep} & \mathrm{T}^{pp} & \cdots \\ \vdots & \vdots & \vdots & \ddots \end{bmatrix}. \qquad (78)$$

The transfer matrices depend on particle yields, $\mathrm{Y}_{\mathrm{ij}}^{\alpha\beta}$, which are defined as the probability of producing a particle of type β in the energy bin j when a primary particle of type α with energy in bin i undergoes an interaction. To calculate $\mathrm{Y}_{\mathrm{ij}}^{\alpha\beta}$ a Monte Carlo simulation can be used (see Protheroe and Johnson (1995) for details).

7.3. Matrix Doubling

From Fig. 12 we see that the smallest effective interaction length is that for synchrotron losses by electrons at high energies. We require δx be much smaller than this distance which is of the order of parsecs for the highest magnetic field considered. To follow the cascade for a distance corresponding to a redshift of $z \sim 9$, and to complete the calculation of the cascade using repeated application of the transfer matrices would require $\sim 10^{12}$ steps. This is clearly impractical, and one must use the more sophisticated approach described below.

The matrix method and matrix doubling technique have been used for many years in radiative transfer problems (van de Hulst 1963, Hovenier 1971). The method described by Protheroe and Stanev (1993) is summarized below. Once the transfer matrices have been calculated for a distance δx, the transfer matrix for a distance $2\delta x$ is simply given by applying the transfer matrices twice, i.e.

$$[\mathrm{T}(2\delta x)] = [\mathrm{T}(\delta x)]^2. \qquad (79)$$

In practice, it is necessary to use high-precision during computation (e.g. double-precision in FORTRAN), and to ensure that energy conservation is preserved after each doubling. The new matrices may then be used to calculate the transfer matrices for distance $4\delta x$, $8\delta x$, and so on. A distance $2^n\delta x$ only requires the application of this 'matrix doubling' n times. The spectrum of electrons and photons after a large distance Δx is then given by

$$[\mathrm{F}(x+\Delta x)] = [\mathrm{T}(\Delta x)][\mathrm{F}(x)] \qquad (80)$$

where $[\mathrm{F}(x)]$ represents the input spectra, and $\Delta x = 2^n\delta x$. In this way, cascades over long distances can be modelled quickly and efficiently.

8. The Origin of Cosmic Rays between 100 TeV and 300 EeV

The highest energy cosmic rays show no major differences in their air shower characteristics to cosmic rays at lower energies. One would therefore expect the highest energy cosmic rays to be protons particularly, if as is most likely, they are extragalactic in origin. However, it is possible that they are not single nucleons. Obvious candidates are heavier nuclei (e.g. Fe), γ-rays and neutrinos. In general it is even more difficult to propagate nuclei than protons, because of the additional photonuclear disintegration which occurs (Tkaczyk et al. 1975, Puget et al. 1976, Karakula and Tkaczyk 1993, Elbert and Sommers 1995, Anchordoqui et al. 1997, Stecker and Salamon 1999). The possibility that the 300 EeV event is a γ-ray has been discussed recently (Halzen et al. 1995) and, although not completely ruled out, the air shower development profile seems inconsistent with a γ-ray primary. Weakly interacting particles such as neutrinos will

have no difficulty in propagating over extragalactic distances, of course. This possibility has been considered, and generally discounted (Halzen et al. 1995, Elbert and Sommers 1995), mainly because of the relative unlikelihood of a neutrino interacting in the atmosphere, and the necessarily great increase in the luminosity required of cosmic sources. Magnetic monopoles accelerated by magnetic fields in our Galaxy have also been suggested (Kephart and Weiler 1996) and can not be ruled out as the highest energy events until the expected air shower development of a monopole-induced shower is worked out.

The subject of possible acceleration sites of cosmic rays at these energies has been reviewed by Hillas (1984) and Axford (1994), and one of the very few plausible acceleration sites may be associated with the radio lobes of powerful radio galaxies, either in the hot spots (Rachen and Biermann 1993) or possibly the cocoon or jet (Norman et al. 1995). One-shot processes such as magnetic reconnection (e.g. in jets or accretion disks) comprise another possible class of sources (Haswell et al. 1992, Sorrell 1987).

Acceleration at the termination shock of the galactic wind from our Galaxy has also been suggested by Jokipii and Morfill (1985), but due to the lack of any statistically significant anisotropy associated with the Galaxy it is unlikely to be the explanation. However, a recent re-evaluation of the world data set of cosmic rays has shown that there is a correlation of the arrival directions of cosmic rays above 40 EeV with the supergalactic plane (Stanev et al. 1995), lending support to an extragalactic origin above this energy, and in particular to models where "local" sources (< 100 Mpc) would appear to cluster near the supergalactic plane. Such a correlation would also be consistent with a Gamma Ray Burst (GRB) origin as several GRB have now been identified with galaxies.

8.1. Active Galactic Nuclei

Rachen and Biermann (1993) have demonstrated that cosmic ray acceleration in Fanaroff-Riley Class II radio galaxies can fit the observed spectral shape and the normalization at 10 – 100 EeV to within a factor of less than 10. The predicted spectrum below this energy also fits the proton spectrum inferred from Fly's Eye data (Rachen et al. 1993). Protheroe and Johnson (1995) have repeated Rachen and Biermann's calculation to calculate the flux of diffuse neutrinos and γ-rays which would accompany the UHE cosmic rays, and their result is shown in Fig. 13. The flux of extremely high energy neutrinos may give important clues to the origin of the UHE cosmic rays. (For a review of high energy neutrino astrophysics see Protheroe 1998)

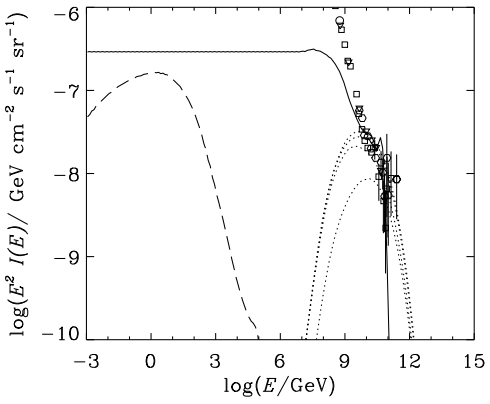

Fig. 13.— Cosmic ray proton intensity multiplied by E^2 in the model of Rachen and Biermann for $H_0 = 75$ km s^{-1} Mpc^{-1} with proton injection up to 3×10^{11} GeV (solid line). Also shown are intensities of neutrinos (dotted lines, $\nu_\mu, \bar{\nu}_\mu, \nu_e, \bar{\nu}_e$ from top to bottom), and photons (long dashed lines). Data are from Stanev (1992); large crosses at EeV energies are an estimate of the proton contribution to the total intensity based on Fly's Eye observations. (From Protheroe and Johnson 1995).

Very recently, Farrar and Biermann (1998) have found a remarkable correlation between the arrival directions of the five highest energy cosmic rays having well measured arrival directions and radio-loud flat spectrum radio quasars with redshifts ranging from 0.3 to 2.2. The probability of obtaining the observed correlation by chance is estimated to be 0.5%. Although the statistical significance is not overwhelming, if further evidence is provided for this correlation the consequences would be far reaching. The distances to these AGN are far in excess of the energy-loss distance for pion photoproduction by protons. Furthermore, given the existence of intergalactic magnetic fields, any charged particle would be significantly deflected and there should be no arrival direction correlation with objects at such distances. Hence, the particles responsible must be stable, neutral, and have a very low cross section for interaction with radiation. Of currently known particles, only the neutrino fits this description, however supersymmetric particles are another possibility. The difficulty of having high energy neutrinos producing the highest energy cosmic rays directly is circumvented if the neutrinos interact well before reaching Earth and produce a particle or particles which will produce a normal looking air shower. Farrar and Biermann (1998) note that, as suggested by Weiler

(1998), this may occur due to interactions with the 1.9 K cosmic background neutrinos. Very recent calculations by Yoshida et al (1998) have shown that as a result of such interactions, and subsequent cascading, a flux of ultra high energy γ-rays would result. The clustering of massive relic light neutrinos in hot dark matter galactic halos would give an even denser nearby target for ultra high energy neutrinos as suggested by Fargion et al. (1997).

8.2. Gamma ray bursts

Gamma ray bursts (GRB) provide an alternative scenario for producing the highest energy cosmic rays (Waxman 1995, Vietri 1995) , and this possibility has received renewed attention following the discovery that they are cosmological. GRB are observed to have non-thermal spectra with photon energies extending to MeV energies, and in some GRB to much higher energies (GRB 940217 was observed by EGRET up to 18 GeV, Hurley et al. 1994). Recent identification of GRB with galaxies at large redshifts (e.g. GRB 971214 at $z = 3.42$, Kulkarni et al 1998) show that the energy output in γ-rays alone from these objects can be as high as 3×10^{53} erg if the emission is isotropic, making these the most energetic events in the Universe. GRB 980425 has been tentatively identified by Galama et al (1998) with an unusual supernova in ESO 184-G82 at a redshift of $z = 0.0085$ implying an energy output of 10^{52} erg. These high energy outputs, combined with the short duration and rapid variability on time-scales of milliseconds, require highly relativistic motion to allow the MeV photons to escape without severe photon-photon pair production losses. The energy sources of GRB may be neutron star mergers with neutron stars or with black holes, collapsars associated with supernova explosions of very massive stars, hyperaccreting black holes, hypernovae, etc. (see Popham et al 1998, Iwamoto et al 1998 for references to these models).

In the relativistic fireball model of GRB (Meszaros and Rees 1994) a relativistic fireball sweeps up mass and magnetic field, and electrons are energized by shock acceleration and produce the MeV γ-rays by synchrotron radiation. Protons will also be accelerated, and may interact with the MeV γ-rays producing neutrinos via pion photoproduction and subsequent decay at energies above $\sim 10^{14}$ eV (Waxman and Bahcall 1997, Rachen and Meszaros 1998). Acceleration of protons may also take place to energies above 10^{19} eV, producing a burst of neutrinos at these energies by the same process (Vietri 1998). These energetic protons may escape from the host galaxy to become the highest energy cosmic rays (Waxman 1995, Vietri 1995). Additional neutrinos due to interactions of the highest energy cosmic rays with the CMBR will be produced as discussed in the previous section.

8.3. Topological defects

Finally, I discuss perhaps the most uncertain of the components of the diffuse high energy neutrino background, that due to topological defects (TD). In a series of papers (Hill 1983, Aharonian et al. 1992, Bhattacharjee et al. 1992, Gill and Kibble 1994) , TD have been suggested as an alternative explanation of the highest energy cosmic rays. In this scenario, the observed cosmic rays are a result of top-down cascading, from somewhat below (or even much below, depending on theory) the GUT scale energy of $\sim 10^{16}$ GeV (Amaldi 1991), down to 10^{11} GeV and lower energies. These models put out much of the energy in a very flat spectrum of neutrinos, photons and electrons extending up to the mass of the "X–particles" emitted.

Protheroe and Stanev (1996) argued that these models appear to be ruled out by the GeV γ-ray intensity produced in cascades initiated by X-particle decay for GUT scale X-particle masses. The γ-rays result primarily from synchrotron radiation of cascade electrons in the extragalactic magnetic field and were found to just exceed the observed diffuse γ-ray background for a magnetic field of 10^{-9} G and X-particle mass of 1.3×10^{14} GeV if the observable particle intensity was normalized to the UHE cosmic ray data. Thus , for such magnetic fields and higher X-particle masses (e.g. GUT scale), TD cannot explain the highest energy cosmic rays. Indeed there is evidence to suggest that magnetic fields between galaxies in clusters could be as high as 10^{-6} G (Kronberg 1994). However, for lower magnetic fields and/or lower X-particle masses the TD models might explain the highest energy cosmic rays without exceeding the GeV γ-ray limit. For example, Sigl et al. (1997) show that a TD origin is not ruled out if the extragalactic field is as low as 10^{-12} G, and Birkel & Sarkar (1998) adopt an X-particle mass of 10^{12} GeV.

I emphasize that the TD model predictions are *not* absolute predictions, but the intensity of γ-rays and nucleons in the resulting cascade is normalized in some way to the highest energy cosmic ray data. It is my opinion that GUT scale TD models are neither necessary nor able to explain the highest energy cosmic rays without violating the GeV γ-ray flux observed. The predicted neutrino intensities are therefore *extremely* uncertain. Nevertheless, it is important to search for such emission because, if it is found, it would overturn our current thinking on the origin of the highest energy cosmic rays and, perhaps more importantly, our understanding of the Universe itself.

9. Observability of Ultra High Energy Gamma Rays

In at least one of the origin models discussed above, a significant fraction of the "observable particles" at 300 EeV are γ-rays, and so it is appropriate to consider the detectability of such energetic photons. Above 100 EeV the interaction properties of γ-rays in the terrestrial environment are very uncertain. Two effects may play a significant role: interaction with the geomagnetic field, and the Landau-Pomeranchuk-Migdal (LPM) effect (Landau and Pomeranchuk 1953, Migdal 1956).

Energetic γ-rays entering the atmosphere will be subject to the LPM effect (the suppression of electromagnetic cross-sections at high energies) which becomes very important at ultra-high energies. The radiation length changes as $(E/E_{\rm LPM})^{1/2}$, where $E_{\rm LPM} = 6.15 \times 10^4 \ell_{\rm cm}$ GeV, and $\ell_{\rm cm}$ is the standard Bethe-Heitler radiation length in cm (Stanev et al. 1982). Protheroe and Stanev (1996) found that average shower maximum will be reached below sea level for energies 5×10^{11} GeV, 8×10^{11} GeV, and 1.3×10^{12} GeV for γ–rays entering the atmosphere at $\cos\theta = 1$, 0.75, and 0.5 respectively. Such showers would be very difficult to reconstruct by experiments such as Fly's Eye and at best would be assigned a lower energy.

Before entering the Earth's atmosphere γ-rays and electrons are likely to interact on the geomagnetic field (see Erber (1968) for a review of the theoretical and experimental understanding of the interactions). In such a case the γ-rays propagating perpendicular to the geomagnetic field lines would cascade in the geomagnetic field, i.e. pair production followed by synchrotron radiation. The cascade process would degrade the γ-ray energies to some extent (depending on pitch angle), and the atmospheric cascade would then be generated by a bunch of γ-rays of lower energy. Aharonian et al. (1991) have considered this possibility and conclude that this bunch would appear as one air shower, having the energy of the initial gamma-ray outside the geomagnetic field, being made up of the superposition of many air showers of lower energy where the LPM effect is negligible. If this is the case, then γ-rays above 300 EeV would be observable by Fly's Eye, etc. There is however, some uncertainty as to whether pair production will take place in the geomagnetic field. This depends on whether the geomagnetic field spatial dimension is larger than the formation length of the electron pair, i.e. the length required to achieve a separation between the two electrons that is greater than the classical radius of the electron (see also Stanev and Vankov 1996).

10. Affect of large-scale magnetic structure

At low energies, propagation of cosmic rays through the Galaxy smears out their arrival directions, giving rise to an almost isotropic distribution. However, simulations of cosmic rays through a model of the galactic magnetic field including a turbulent component shows that for energies greater than ∼Z EeV significant anisotropies may be expected from sources in our Galaxy (see, e.g., Lee and Clay 1995). Clearly, at much higher energies the magnetic field of our galaxy plays an insignificant role in smearing directions of extragalactic cosmic ray nuclei. Ultra-high energy cosmic rays can be subject, however, to significant deflection and energy dependent time delays in large scale extragalactic or halo magnetic fields. Lemoine et al. (1997) have performed Monte Carlo simulations of propagation which show how the duration of cosmic ray emission in distant sources has a dramatic effect on the observed spectrum. For example, in one model, a bursting source at 30 Mpc with an E^{-2} spectrum gave a spectrum very strongly peaked at 110 EeV.

Ryu et al. (1998) consider the possibility that the cosmic magnetic field, instead of being uniformly distributed, is strongly correlated with the large scale structure of the Universe. They derive an upper limit to the magnetic field in filaments and sheets of $1\mu G$ which is $\sim 10^3$ times higher than the previously quoted values. Clearly, if such cosmic structures have high magnetic fields this will have important consequences for cosmic ray acceleration and propagation. For example, Tanco (1998b) has considered propagation through well ordered compressed magnetic fields ($\sim 0.1\mu$G) inside cosmological walls and found the cosmic ray flux leaving a wall to be highly anisotropic (by 2 or 3 orders of magnitude), being greatest near the central perpendicular of the wall. Thus, we might expect an anisotropy in the direction perpendicular to the nearest cosmological wall (Centaurus). He also found that arrival directions of CR are smeared, and correlations between γ-rays and CR in bursting events are lost.

Sigl, Lemoine and Biermann (1998) have considered propagation in the local supercluster with $B_{\rm rms} \sim 0.1\mu$G, with a maximum eddy length of 10 Mpc and a distance to the nearest source of 10 Mpc. For a soft injection spectrum, $E^{-2.4}$, and with both the source and the observer in the local supercluster (sheet with thickness 10 Mpc) they found excellent agreement with the spectrum observed above 10 EeV. Below 100 EeV cosmic rays diffuse, with arrival directions at Earth being spread out over $\sim 80^\circ$ while above 200 EeV they are just deflected but still have a significant spread in arrival directions of $\sim 10^\circ$ explaining the lack of correlation of the highest energy

cosmic ray with any known nearby source. Tanco (1998a) noted that the local distribution of luminous matter is far from uniform, and using a redshift distribution based on the CfA redshift catalog they found agreement with the observed super-GZK spectrum. A similar conclusion was reached by Blasi and Olinto (1998).

11. Conclusion

While the origin of the highest energy cosmic rays remains uncertain, there appears to be no necessity to invoke exotic models. Shock acceleration, which is believed to be responsible for the cosmic rays up to at least 100 GeV, is a well-understood mechanism and there is evidence of shock acceleration taking place in radio galaxies (Biermann and Strittmatter 1987), and the conditions there are favourable for acceleration to at least 300 EeV. Such a model, in which cosmic rays are accelerated in Fanaroff-Riley Class II radio galaxies, can readily account for the flat component of cosmic rays which dominates the spectrum above ~ 10 EeV (Rachen et al. 1993). Indeed, one of the brightest FR II galaxies, 3C 134, is a candidate source for the 300 EeV Fly's Eye event (Biermann, 1997).

Whatever the source of the highest energy cosmic rays, because of their interactions with the radiation and magnetic fields in the Universe, the cosmic rays reaching Earth will have spectra, composition and arrival directions affected by propagation. In particular the composition of the arriving particles may differ drasticly from that on acceleration. For example, the accompanying fluxes of neutrinos produced in the sources and by cascade processes during propagation to Earth may dominate the spectrum at highest energies. The astrophysics ingredients to the propagation (e.g., magnetic field intensities and configurations) are still somewhat uncertain, and we need better statistics on the arrival directions, energy spectra and composition, as well as the intensity of the diffuse backgrounds of very high energy neutrinos and γ-rays (partly produced in cascades initiated by cosmic ray interactions).

The Auger Project (Auger Collaboration 1995), an international collaboration to build two UHE cosmic ray detectors, one in the United States and one in Argentina, each having a collecting area of about 3000 km^2 , and will measure the energy spectrum and anisotropy of the highest energy cosmic rays with the required precision, and will also be sensitive to extremely high energy neutrinos (Capelle et al. 1998). The next generation neutrino telescopes, such as the planned extension of AMANDA, ICECUBE (Shi et al 1998), and ANTARES (Blanc et al. 1997), may have effective areas of 0.1 km^3, or larger, and be sufficiently sensitive to detect bursts of neutrinos from extragalactic objects and to map out the spectrum of the diffuse high energy neutrino background.

Once we have better better statistics of particle fluxes we will be better placed to understand the origin of the highest energy particles occurring in nature. Furthermore, once the astrophysics is worked out, cosmic rays will be the tool for exploring particle physics well above terrestrial accelerator energies.

Acknowledgments

This chapter is based in part on a lecture given at Erice (Protheroe 1996). I thank Qinghuan Luo, Anita Mücke and Peter Biermann for reading the manuscript. My research is supported by a grant from the Australian Research Council.

REFERENCES

Aharonian, F.A., Kanevsky, B.L., and Sahakian, J., *J. Phys. G*, **17** (1991) 1909.

Aharonian, F.A., Bhattacharjee, P., and Schramm, D., *Phys. Rev. D* **46** (1992) 4188.

Allen, G.E., et al., *Astrophys. J. Lett.* **487** (1997) 97

Amaldi, U., de Boer, W., and Fürstenau, H., *Phys. Lett.* **B260** (1991) 447.

Anchordoqui, L.A., Dova, M.T., Epele, L.N., Swain, J.D., *Phys. Rev. D* **57** (1998) 7103.

Auger Collaboration, "The Pierre Auger Project Design Report" (Fermilab 1995).

Axford, W.I., *Ap. J. Suppl.* **90** (1994) 937.

Axford, W.I., Lear, E., and Skadron, G., *Proc. 15th Int. Cosmic Ray Conf., Plovdiv*, **11** (1977) 132.

Axford W.I. *Astrophysical Aspects of Cosmic Rays* ed. M. Nagano and F. Takahara (World Scientific, Singapore, 1991) p. 46.

Baring, M.G., Proc. of XXXIInd Rencontres de Moriond, "Very High Energy Phenomena in the Universe", eds. Giraud-Heraud, Y. & Tran Thanh Van, J., (Editions Frontieres, Paris, 1997), p. 97.

Baring, M.G., Ellison, D.C., Reynolds, S.P., Grenier, I., and Goret, P., *Ap. J.* **513** (1999) in press. astro-ph/9810158

Bednarz, J., Ostrowski, M., *Mon. Not. R. Astr. Soc.*, **283** (1996) 447.

Bednarz, J., Ostrowski, M., *Phys. Rev. Lett.* **80** (1998) 3911.

Bednarz, J., "Proceedings of 16th Europ. Cosmic Ray Symp.", in press (1998).

Bell, A.R., *Mon. Not. R. Astr. Soc.*, **182** (1978) 443.

Berezhko, E.G., and Krymski, G.F., *Usp. Fiz. Nauk* **154** (1988) 49.

Berezinsky, V.S. and Grigor'eva, S.I., *Astron. Astrophys.* **199** (1988) 1.

Berezinsky, V.S., *Yad. Fiz.* **11** (1970) 339; English translation in *Sov. J. Nucl. Phys.*, **11** (1970) 222.

Bhattacharjee, P., Hill, C.T., and Schramm, D.N., *Phys. Rev. Lett.* **69** (1992) 567.

Biermann, P.L., and Strittmatter, P.A., *Ap. J.* **322** (1987) 643.

Biermann, P.L., and Cassellini, J.P., *Astron. Astrophys.* **277** (1993) 691.

Biermann, P.L., *J. Phys. G: Nucl. Part. Phys.* **23** (1997) 1.

Bird, D.J., *et al.*, *Ap. J.* **424** (1994) 491.

Bird, D.J., *et al.*, *Ap. J.* **441** (1995) 144.

Birkel, M., and Sarkar, S., preprint (1998) hep-ph/9804285

Blanc, F., et al., ANTARES proposal (1997) astro-ph/9707136

Blandford, R.D., and Ostriker, J.P., *Astrophys. J. Lett.* **221** (1978) L29.

Blandford, R, and Eichler, D., *Phys. Rep.* **154** (1987) 1.

Blasi, P., Olinto, A.V., submitted to *Phys. Rev. D* (1998) astro-ph/9806264

Brazier, K.T.S., Kanbach, G., Carraminana, A., Guichard, J., and Merck, M., *Mon. Not. R. Astr. Soc.*, **281** (1996) 1033.

Brecher, K., and Burbidge, G.R., *Ap. J.* **174** (1972) 253.

Bridle, A.H., *Mon. Not. R. Astron. Soc.* **136** (1967) 14.

Capelle, K.S., Cronin, J.W., Parente, G., Zas, E., *Astropart. Phys.* **8** (1998) 321.

Clarke, T.A., Brown, L.W. and Alexander, J.K., *Nature* **228** (1970) 847.

Dawson, B.R., Meyhandan, R., Simpson, K.M., *Astropart. Phys.* in press (1998) astro-ph/9801260 .

Donea, A.C., and Biermann, P.L., (1996) personal communication.

Drury, L.O'C., *Space Sci. Rev.* **36** (1983) 57.

Drury, L.O'C., *Rep. Prog. Phys.* **46** (1983) 973.

Drury, L.O'C., Aharonian, F.A., and Völk, H.J., *Astron. Astrophys.* **287** (1994) 959.

Elbert, J.W., and Sommers, P., *Ap. J.* **441** (1995) 151.

Ellison, D.C, Jones, F.C., Reynolds, S.P., *Ap. J.* **360** (1990) 702.

Ellison, D.C, Eichler, D., *Ap. J.* **286** (1984) 691.

Epele, L.N., Roulet, E., *J. High Energy Phys.* **9810** (1998) 9.

Erber, T., *Phys. Rev.* **38** (1968) 626.

Esposito, J.A., Hunter, S.D., Kanbach, G., and Sreekumar, P., *Astrophys. J.* **461** (1996) 820.

Fargion, D., Mele, B., Salis, A., (1997) astro-ph/9710029

Farrar, G.R., and Biermann P.L., *Phys. Rev.* **81** (1998) 3579.

Fletcher, R.S., Gaisser, T.K., Lipari, P., Stanev, T., *Phys. Rev. D* **50** (1994) 5710.

Gaisser, T.K., *Cosmic Rays and Particle Physics*, (Cambridge University Press, Cambridge, 1990).

Gaisser, T.K., Protheroe, R.J., and Stanev, T., *Astrophys. J.* **492** (1998) 219.

Galama, T.J., et al., *Nature*, **395** (1998) 670 astro-ph/9806175

Gill, A.J., and Kibble, T.W.B., *Phys. Rev. D* **50** (1994) 3660.

Greisen, K., *Phys. Rev. Lett.* **16** (1966) 748.

Hayashida, N., *et al.*, *Phys. Rev. Lett.* **73** (1994) 3491.

Hayashida, N., *et al.*, preprint (1998) astro-ph/9807045

Halzen F., Vazquez R.A., Stanev T. and Vankov H.P., *Astroparticle Phys.*, **3** (1995) 151.

Halzen, F., 18th Int. Conf. on Neutrino Phys. and Astrophys. (Neutrino 98), Takayama, Japan (1998) hep-ex/9809025

Haswell, C.A., Tajima, T., and Sakai, J.-L., *Ap. J.* **401** (1992) 495.

Hill, C.T., *Nucl. Phys. B* **224** 469 (1983)

Hill, C.T., and Schramm, D.N., *Phys. Rev. D* **31** (1985) 564.

Hillas, A.M, *Ann. Rev. Astron. Astrophys.* **22** (1984) 425.

Hovenier, J.V., *Astron. Astrophys.* **13** (1971) 7.

van de Hulst, H.C., *A New Look at Multiple Scattering*, Report, NASA Institute for Space Studies, New York, 1963).

Hurley, K., et al., *Nature*, **372** (1994) 652.

Ip, W.-H., and Axford, W.I., in *Particle Acceleration in Cosmic Plasmas*, eds. T.K. Gaisser and G.P. Zank (AIP Conference Proceedings No. 264, 1991) p. 400.

Iwamoto, K., et al., *Nature*, **395** (1998) 672

Jokipii, J.R., and Morfill G.E., *Ap. J. Lett.* **290** (1985) L1.

Jokipii, J.R., *Astrophys. J.* **313** (1987) 842.

Jones, F.C., and Ellison, D.C., *Space Sci. Rev.* **58** (1991) 259.

Karakula, S., and Tkaczyk, W., *Astroparticle Phys.* **1** (1993) 229.

Kephart, T.W., and Weiler, T.J., *Astroparticle Phys.*, **4** (1996) 271.

Kirk, J.G., Schneider, P., *Ap. J.* **315** (1987) 425.

Koyama, K., Petre, R., Gotthelf, E.V., Hwang, U., Matsura, M., Ozaki, M., and Holt, S.S., *Nature* **378** (1995) 255.

Kronberg, P.P., *Rep. Prog. Phys.* **57** (1994) 325.

Krymsky, G.F., *Dokl. Akad. Nauk. SSSR*, **243** (1977) 1306.

Kulkarni, S.R., et al., *Nature*, **393** (1998) 35

Lagage, P.O., and Cesarsky, C.J., *Astron. Astrophys.* **118** (1983) 223

Landau, L.D., and Pomeranchuk, I., *Dok. Akad. Nauk. SSSR* **92** (1953) 535.

Lee, A.A., and Clay, R.W., *J. Phys. G: Nucl. Part. Phys.* **21** (1995) 1743.

Lemoine, M., Sigl, G., Olinto, A.V.,Schramm, D.N., *Astrophys. J. Lett.* **486** (1997) L115.

Mannheim, K., Rachen, J.P., Protheroe, R.J., in preparation (1998)

Markiewicz W.J., Drury L. O'C., and Volk H.J., *Astron. Astrophys.* **236** (1990) 487.

Mastichiadis, A., Protheroe, R.J. and Szabo, A.P. *Mon. Not. R. Astron. Soc.* **266** (1994) 910.

Mastichiadis, A., *Astron. Astrophys.*, **305** (1996) 53.

Melrose, D.B., and Crouch, A.D., *Publ. Astron. Soc. Aust.* **14** (1997) 251.

Meszaros, P., and Rees, M., *Mon. Not. R. Astr. Soc.* **269** (1994) 41P

Mücke, A., Rachen, J.P., Engel, R., Protheroe, R.J., Stanev, T., *Publ. of the Astron. Soc. of Australia*, submitted (1998) astro-ph/9808279

Migdal, A.B., *Phys. Rev.* **103** (1956) 1811.

Norman, C.A., Melrose, D.B., and Achterberg, A., *Astrophys. J.* **454** (1995) 60.

Ostrowski, M., Proc. Vulcano Workshop 1998: "Frontier Objects in Astrophysics and Particle Physics", in press (1998).

Popham, R., Woosley, S.E., and Fryer, C., *Ap. J.*, submitted (1998) astro-ph/9807028

Protheroe, R.J., and Stanev, T.S., *Mon. Not. R. Astron. Soc.* **264** (1993) 191.

Protheroe, R.J., Stanev, T., and Berezinsky, V.S., *Phys. Rev. D15*, **151** (1995) 4134.

Protheroe, R.J., and Biermann, P.L., *Astroparticle Phys.*, **6** (1996) 45.

Protheroe, R.J., *Mon. Not. R. Astron. Soc.* **221** (1986) 769.

Protheroe, R.J., *Mon. Not. R. Astr. Soc.* **246** (1990) 628.

Protheroe, R.J., Mastichiadis A. and Dermer C.D. *Astroparticle Phys.* **1** (1992) 113.

Protheroe, R.J., and Johnson, P.A., *Astroparticle Phys.* **4** (1995) 253 and erratum **5** (1996) 215.

Protheroe, R.J., and Stanev, T., *Phys. Rev. Lett.* **77** (1996) 3708, and Erratum **78**, 3420 (1997)

Protheroe, R.J., in Towards the Millennium in Astrophysics: Problems and Prospects, Erice 1996, eds. M.M. Shapiro and J.P. Wefel (World Scientific, Singapore), in press. astro-ph/9612212

Protheroe, R.J., and Stanev, T., *Astroparticle Phys.*, in press (1998) astro-ph/9808129

Protheroe, R.J., 18th Int. Conf. on Neutrino Phys. and Astrophys. (Neutrino 98), Takayama, Japan (1998) astro-ph/9809144

Puget, J.L., Stecker, F.W., Bredekamp, J.H., *Ap. J.* **205** (1976) 638.

Rachen, J.P., Stanev, T., and Biermann, P.L., *Astron. Astrophys.* **273** (1993) 377.

Rachen, J.P., and Biermann, P.L., *Astron. Astrophys.* **272** (1993) 161.

Rachen, J.P., and Meszaros, P., *Phys. Rev. D*, **58** (1998) 12-30-05 astro-ph/9802280

Reynolds, S.P., *Astrophys. J. Lett.* **459** (1996) L13.

Ressell, M.T., and Turner, M.S., *Comm. Astrophys.* **14** (1990) 323.

Ryu, D., Kang, H., and Biermann, P.L., *Astron. Astrophys.* **335** (1998) 19.

Shi, X., Fuller, G.M., Halzen, F., submitted to *Phys. Rev. Lett.* (1998) astro-ph/9805242

Sigl, G., Lee, S., Schramm, D., and Coppi, P., *Phys. Lett. B* **392** (1997) 129.

Sigl, G., Lemoine, M., Biermann, P.L., *Astropart. Phys.* in press (1998) astro-ph/9806283

Sorrell, W.H., *Ap. J.* **323** (1987) 647.

Stanev, T., Biermann, P.L., Lloyd-Evans, J., Rachen, J.P., and Watson, A.A., *Phys. Rev. Lett.* **75** (1995) 3056.

Stanev, T., in *Particle Acceleration in Cosmic Plasmas*, edited by G.P. Zank and T.K. Gaisser (American Institute of Physics, New York, 1992) p. 379.

Stanev, T., et al., *Phys. Rev. D* **25** (1982) 1291.

Stanev, T., and Vankov, H.P., *Phys. Rev. D.* **55** (1996) (1997) 1365.

Stecker, F.W., "Cosmic Gamma Rays" (Baltimore: Mono Book Co., 1971) p. 133.

Stecker, F.W., and Salamon, M., *Ap. J.* **512** (1999) in press.

Szabo, A.P., and Protheroe, R.J., *Astropart. Phys.* **2** (1994) 375.

Takeda, M., et al., *Phys. Rev. Lett.* **81** (1998) 1163.

Tanco, G.M., *Astrophys. J. Lett.* (1998a) astro-ph/9810366

Tanco, G.M., *Astrophys. J. Lett.* **505** (1998b) 79

Tanimori, T., et al. *Ap. J. Lett.* **497** (1998) 25

Tkaczyk, W., Wdowczyk, J., and Wolfendale, A.W., *J. Phys. A* **8** (1975) 1518.

Totani, T., submitted to *Phys. Rev. Lett.* astro-ph/9810207

Vietri, M., *Ap. J.*, *453* (1995) 883.

Vietri, M., *Phys. Rev. Lett.* **80** (1998) 3690

Waxman, E., *Phys. Rev. Lett.* **75** (1995) 386

Waxman, E., and Bahcall, J., *Phys. Rev. Lett.* **78** (1997) 2292.

Waxman, E., and Bahcall, J., *Phys. Rev. D* submitted (1998) hep-ph/9807282

Weiler, T., *Astroparticle Phys.*, in press (1998) hep-ph/9710431

Yoshida, S., Sigl, G., Lee, S., *Phys. Rev. Lett.* submitted (1998) hep-ph/9808324

Zatsepin, G.T., and Kuz'min, V.A., *JETP Lett.* **4** (1966) 78.

This 2-column preprint was prepared with the AAS LaTeX macros v4.0.